Progress In Electromagnetics Research M, Vol. 92, 89–101, 2020

Design of Universal Optical Logic Gates Using Heterogeneous Swastika Structured Hexagonal Photonic Crystal Ring Resonator

Damodaran Saranya and Anbazhagan Rajesh*

Abstract—In this paper, a novel heterogeneous swastika structured hexagonal photonic crystal ring resonator for the realization of universal logic gates is designed using two dimensional photonic crystals. The proposed structure has square lattice of 16×16 hexagon-shaped chalcogenide glass rods embedded in an air substrate with a refractive index of 3.1. The choice of chalcogenide in the realization of optical logic gates benefits from wide optical windows in the mid-infrared region. Through plane wave expansion method, the contrast ratio for the proposed structures, namely, NAND, NOR, EX-OR, and EX-NOR gate is 22.6 dB, 17.20 dB, 18.3 dB, and 12.78 dB, respectively. Moreover, the footprint of the proposed structure is $9.24\,\mu m \times 9.24\,\mu m$.

1. INTRODUCTION

In the last few decades, demand for fast and efficient circuits in integrated circuit industry has been developed. Photonic crystals are ordered nanostructures with different dielectric constants arranged in aperiodic form. dielectric structures are designed to influence the propagation of electromagnetic waves. Photonic crystal can be periodic dielectric medium that prevents the flow of light in certain frequencies and can be used in various communication applications. Depending on the geometry of the structure, photonic crystal can be divided into three categories as One Dimension (1D), Two Dimension (2D), and Three Dimension (3D) structures [1]. Two dimensional structures have attracted more because the fabrication process is similar to planar integration circuits. Two-dimensional structure in photonic crystals provides the implementation of fast devices such as waveguides, resonator, switches, and logic gates. Photonic band gaps provide guiding and engineering of the flow of light. Total compactness of the Photonic Crystal (PC) structure makes it suitable for optical integrating.

Recently, all optical logic gates have been attracting wide attention because of their potential application in fields of optical computing systems, optical interconnection, and optical signal processing. Photonic band gaps which are produced in photonic crystals are used in the realization of photonic integrated devices. Photonic crystals [2] have the inherent capacity for the attainment of all optical devices. Waveguide is formed by creating defects in the photonic crystals, and the light is controlled through it. Between the beams, phase difference is employed which is responsible for the positive and negative interference in the logic gates [3]. Theoretical realization on light beam interference effect is studied. Low power is used in the operation. All optical logic gates, OR, XOR, XNOR, NOT, and NAND, are realized with low power, and the contrast ratio between the logic states is 20 dB. For the operation of these logic gates, high power is not necessary. [4]. At particular wavelength, high extinction ratio of more than 3 dB is achieved for XOR and NOT gates. They are capable of operating with multiple wavelengths [5].

Based on the theory of light beam interference effect, reconfigurable structure is designed with no phase difference between the inputs [6]. All optical switches based on nonlinear Phc structure are proposed. A Gallium Arsenide (GaAs) substrate is used based on the threshold logic concept [7]. A

Received 22 January 2020, Accepted 6 April 2020, Scheduled 8 May 2020
* Corresponding author: Anbazhagan Rajesh (rajeshtechece@gmail.com).
The authors are with the School of Electronics and Engineering, VIT University, Vellore, India.

T-branch combiner is designed and investigated using coupled mode theory, and it leads to maximum power at the output [8]. Simulation results show that logic gates are simple and efficient devices for the realization of photonic integrated circuits. In [9], XOR gate is proposed. ring resonators are tilted to 45° before the output to improve the gate efficiency. This photonic gate can be used in electronics, data processing, and cryptography.

Photonic crystal based optical devices exist in the following literature such as optical filter [10–12], optical decoder [13, 14], and asymmetric reflector [15]. A quasi square ring resonator based on eight channel demultiplexers is proposed. The functional characteristics of eight channel demultiplexers are investigated [16]. Using the interference effect, an ultra-fast optical half adder is designed with two-dimensional photonic crystals [17]. Optical reversible gates are proposed based on electromagnetic scattering. The maximum time delay for the proposed structure is 10 ps [18]. Analog to Digital Converter (ADC) based on Kerr effect is proposed. Sampling and quantizing are done at the wavelength of 1550 nm. It can support sampling rate up to 300 GS/s with precision of 1200 KS [19]. Band gap structure, field distribution, and direction of propagation in the two-dimensional photonic crystal waveguide are studied [20].

The main contribution of the paper is as follows. Firstly, a novel ring resonator, which effectively couples the light between the ports of the device, is designed using heterogeneous arrangement of photonic crystals. Here, the photonic crystal is hexagonally structured as compared to the conventional circle or square structure. The hexagon structure is arranged in a square lattice pattern that results in the efficient coupling of the light between the ports. The design has been chosen after carrying out parametric analysis with the choice of lattice and the structure. This novel design displays a high contrast ratio with low footprint. Secondly, the ports of the design follow a swastika profile, and this results in a faster response time than the devices in literature. Finally, using the heterogeneous swastika structured hexagonal photonic crystal ring resonator (PCRR), the universal gates, namely, NAND, NOR, EX-OR, and EX-NOR are designed by controlling the control input of the ring resonator. The realised universal gates exhibit good contrast ratio with reduced footprint.

The rest of the paper is organised as follows. Section 2 discusses the numerical methods in modelling the gates and the design of the proposed NAND, NOR, EX-OR, and EX-NOR structure. In Section 3, simulations and results are discussed and analysed, and finally the concluding remarks are given in Section 4.

2. NUMERICAL METHODS AND MODELLING

Photonic crystals are periodic dielectric structures designed to influence the electromagnetic waves in the same way as the periodic potential in the semiconductor crystals influences the electron motion. This leads to the development of a band structure for photons in photonic crystals. This band gap does not allow certain frequencies, and the defects are introduced artificially using line and point defects. To define the behaviour of light in the photonic crystals, Maxwell equations are considered. Let us assume that the Maxwell equations impose on a field patterns that happens to vary sinusoidal with the time, and the time dependence of electric and magnetic fields is

$$H(r,t) = H(r)e^{-i\omega t} \tag{1}$$

$$E(r,t) = E(r)e^{-i\omega t} \tag{2}$$

where ω refers to the angular frequency. Then the Maxwell equations in the steady state are

$$\nabla \times H(r) + i\omega(\varepsilon(r)\varepsilon_0 E(r)) = 0 \tag{3}$$

$$\nabla \times E(r) = i\omega(\mu_0 H(r)) \tag{4}$$

The above equation is decoupled, and the result in the equation in $H(r)$ is given by:

$$\nabla \times \left(\frac{1}{\varepsilon(r)}\nabla \times H(r)\right) = \left(\frac{\omega}{c}\right)^2 H(r) \tag{5}$$

where $H(r)$ is the eigen vector, and $((\omega/c)^2$ refers the eigen value with ω as the angular frequency. This is referred to the master equation. Let $\Theta = \nabla \times (\frac{1}{\varepsilon(r)})\times$, then the master Equation (5) becomes

$$\Theta H(r) = \left(\frac{\omega}{c}\right)^2 \tag{6}$$

2.1. Band Structure Calculation

To calculate the photonic band structure, plane wave expansion method is used, and it has very high computation. Using this method, band structures for the point defect, line defect, and surface defects are calculated. Maxwell equations in the form of eigen value of electric (E) or magnetic (M) field are expressed as follows,

$$\nabla^2 E = -\left(\frac{\omega}{c}\right)^2 \varepsilon E \tag{7}$$

$$\nabla \times \left(\frac{1}{\varepsilon}\nabla\times\right) H = \left(\frac{\omega}{c}\right)^2 H \tag{8}$$

where ε is the dielectric constant, and it depends on the frequency and speed of light (c).

2.2. Physical and Numerical Parameters

To use the FDTD algorithm, the propagation of light field in the structure is studied using the refractive index distribution $n(x, y, z)$, and any other relevant material properties of the structure itself must be specified.

$$D = \varepsilon_0\varepsilon_\infty E + \varepsilon_r(\omega)\cdot\varepsilon_0 E + 2\varepsilon_0 n n_2 \frac{1}{1+\dfrac{I}{I_{Sat}}} E \tag{9}$$

This equation has three terms, and it corresponds to an individual effect. The initial term takes into account the linear index of the system. The next term takes into account material dispersion, or the change of index as a function of wavelength. The final term in this equation is a nonlinear term and is a function of the intensity in the medium. The electromagnetic waves propagate in (x, z) plane, and the magnetic field is polarized parallel to the y-axis. Typically, the grid spacing must be able to resolve the wavelength in time, and therefore usually less than $\lambda/10$. Here, x and z refer to the coordinators in horizontal and vertical directions, respectively. Since the FDTD algorithms is based on time domain, the temporal and spatial grid size is followed using the condition as follows [13, 14].

$$c\,\Delta t \leq \frac{1}{\sqrt{\dfrac{1}{\Delta x^2}+\dfrac{1}{\Delta z^2}}} \tag{10}$$

where Δt is the step time; c is the velocity of light in free space; and Δx and Δz are space steps along x and z-axes, respectively. In optical logic gates, the light intensity of the signal is used to define the logic '0' and logic '1'. In the output port, logic '0' is considered when there is no light signal, and logic '1' is considered when light intensity is present. The negligible intensity as *logic '0'* at the output results in a very high contrast ratio, and the contrast ratio (CR) is given as

$$\mathrm{CR} = 10\,\log\frac{P_1}{P_0} \tag{11}$$

where P_1 and P_0 are the output power levels of logic '1' and logic '0', respectively.

2.3. FDTD Method

Finite-difference time-domain (FDTD) method is one of the most frequently used computational techniques for simulation of electromagnetic phenomena. Based on central difference approximations in space and time of Maxwell's equations, it provides a direct solution of time-dependent electromagnetic fields in a region of the space. When one looks at the Maxwell's equations, the change in the E-field in time (the time derivative) is dependent on the change in the H-field across space (the curl). This results in the basic FDTD time-stepping relation that, at any point in space, the updated value of the E-field in time is dependent on the stored value of the E-field and the numerical curl of the local distribution of H-field in space. The H-field is time-stepped in a similar manner. Iterating the E-field and H-field updates result in a marching-in-time process in which data analogue to the continuous electromagnetic

waves considered propagate in a numerical grid stored in the computer memory. This description holds true for 1D, 2D, and 3D techniques [20]

In our design, the system is divided into two meshes as Transverse Electric (TE) and Transverse Magnetic (TM) modes. In the simulations, periodic boundary condition is used. Yee's mesh method (also known as Yee lattice) is used to solve the Maxwell equations, which computes the E and H field components at points on a grid with grid points spaced Δx, Δy, and Δz. Furthermore, 16 mesh points in one pitch (period) is set in X and Z axes. However, there are several distinct approaches for solving differential equations. The leap-frog method in literature is efficient for simple structures. However, for complicate structures with line and point defects, the calculation of numerical curl using leap-frog becomes complicated [21].

2.4. Design of Heterogeneous Swastika Structured Hexagonal Photonic Crystal Ring Resonator

The proposed structure haing a swastika-shaped resonator structure is proposed for the universal logic gates, which is designed and analysed. The structure has 16×16 hexagonal shaped square lattice chalcogenide glass rods with a refractive index of 3.1 in X-Z directions. To calculate the optical behaviour of the proposed structure Photonic Bandgap (PBG) is used. The distance between two adjacent rods is 600 nm which is nothing but a lattice constant 'a', and the radius of rod, 'r', is $0.2a$. The photonic band gap for the proposed structure is $0.3034 \leq a/\lambda \leq 0.42566$ which is equal to the wavelength of 0.1105 nm to 1551 nm. The resonant wavelength of the proposed structure is 1550 nm. The basic view of the structure looks the same, but the resonator part alone varies from gate to gate. The proposed structure for NAND, NOR, EX-OR, and EX-NOR, sectional view of the proposed structure, and 3D view of the proposed structures are shown. The photonic band gap of the proposed structure is shown in Fig. 1. Photonic crystals provide a new platform for miniaturised integrated optical circuits and offer new functionalities in dispersion engineering and Wavelength Division Multiplexing (WDM) components.

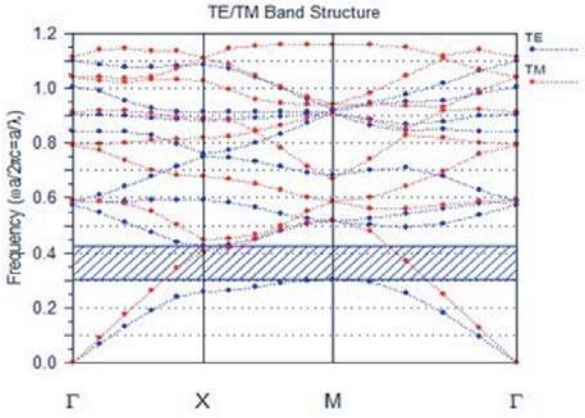

Figure 1. Band diagram of the proposed heterogeneous swastika structured hexagonal photonic crystal ring resonator.

3. PROPOSED STRUCTURE FOR UNIVERSAL GATES USING HETEROGENEOUS SWASTIKA STRUCTURED PCRR

The simulation parameters to design the various universal gates is displayed in Table 1. In NAND gate, the structure has 16×16 hexagonal rods in X-Z directions. The proposed NAND gate structure is shown in Fig. 2. The resonator part has two rings, outer octagonal ring and inner circular ring. The inner ring has the radius of $0.2a$, and the outer rings have blue and orange colour rods with the radii of $0.12a$ and $0.07a$, respectively. The remaining rods in the outer ring have the radius of $0.1a$. It has

Table 1. Design parameters for the realization of universal gates.

Parameters	Symbol	Value	Unit
Resonant wavelength (Λ_0)		1550	nm
Photonic Band gap (TE)	λ	1105–1551	nm
Lattice constant (a)	a	600	nm
Lattice pattern	-	Square	-
Photonic crystal structure	-	Hexagon	-
Background index	n_b	1	-
Lattice rod's refractive index	n_r	2.1	-
Radius of lattice rods	r	120	nm

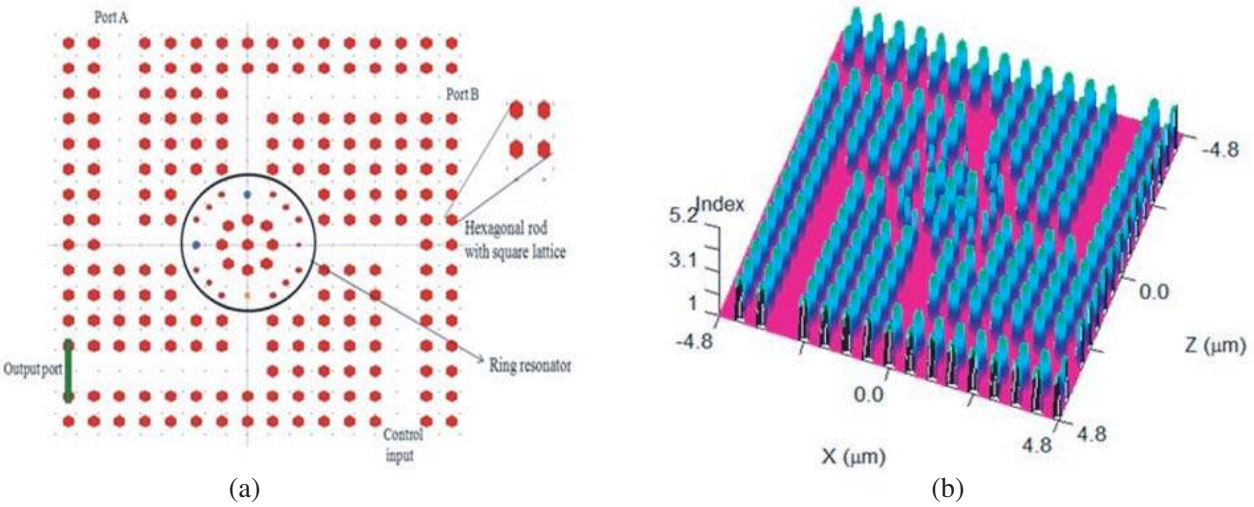

Figure 2. (a) Proposedoptical NAND gate structure, (b) 3D view of the structure.

three inputs as port A, port B, Control Input, and one output. The Control Input (CI) is not active all the time. When both the inputs A and B are given, the phases of 270° and 180° are applied on the input side to get the results.

The truth table for the optical NAND gate is tabulated in Table 2. The transmission diagram and output power for the combinations '00', '01', '10', and '11' of NAND gate are shown in Figure 3. When the Control Input signal is applied and no light signal from port 'A' and port 'B', the output power of $0.558P_a$ is obtained which is considered as logic-1. When there is no signal from port 'A' and signal at port 'B', the output power obtained is $0.672\mathrm{P}_a$ which is also considered to be logic-1. When the signal from port 'A' is applied and no signal at port 'B', the output power is $0.952P_a$ which is considered to be logic-1. But among the three combinations, the high output power is $0.952P_a$ which is obtained for the combination '10', so finally this is considered to be logic-1. When both the inputs are given, the output power of $0.005P_a$ is obtained, and this is considered to be logic-0. The ON-OFF extinction ratio of NAND gate is obtained from the output transmission of logic '0' and logic '1'.

In NOR gate, the proposed structure has three inputs, Port A, Port B, Control Input, and one output. The resonator part has two rings, outer square ring and inner circular ring. The proposed structure is shown in Fig. 4. The inner ring rods have the radius of $0.2a$. The outer ring acts as coupling rods with the radius of $0.07a$. The orange, blue, and grey colour scattered rods have the radii of $0.12a$, $0.1a$, and $0.09a$, respectively. The scattered rods are used to avoid leakage, and the coupling rods are used to couple the input signal. The control input is active only when $A = 0$, $B = 0$, and the

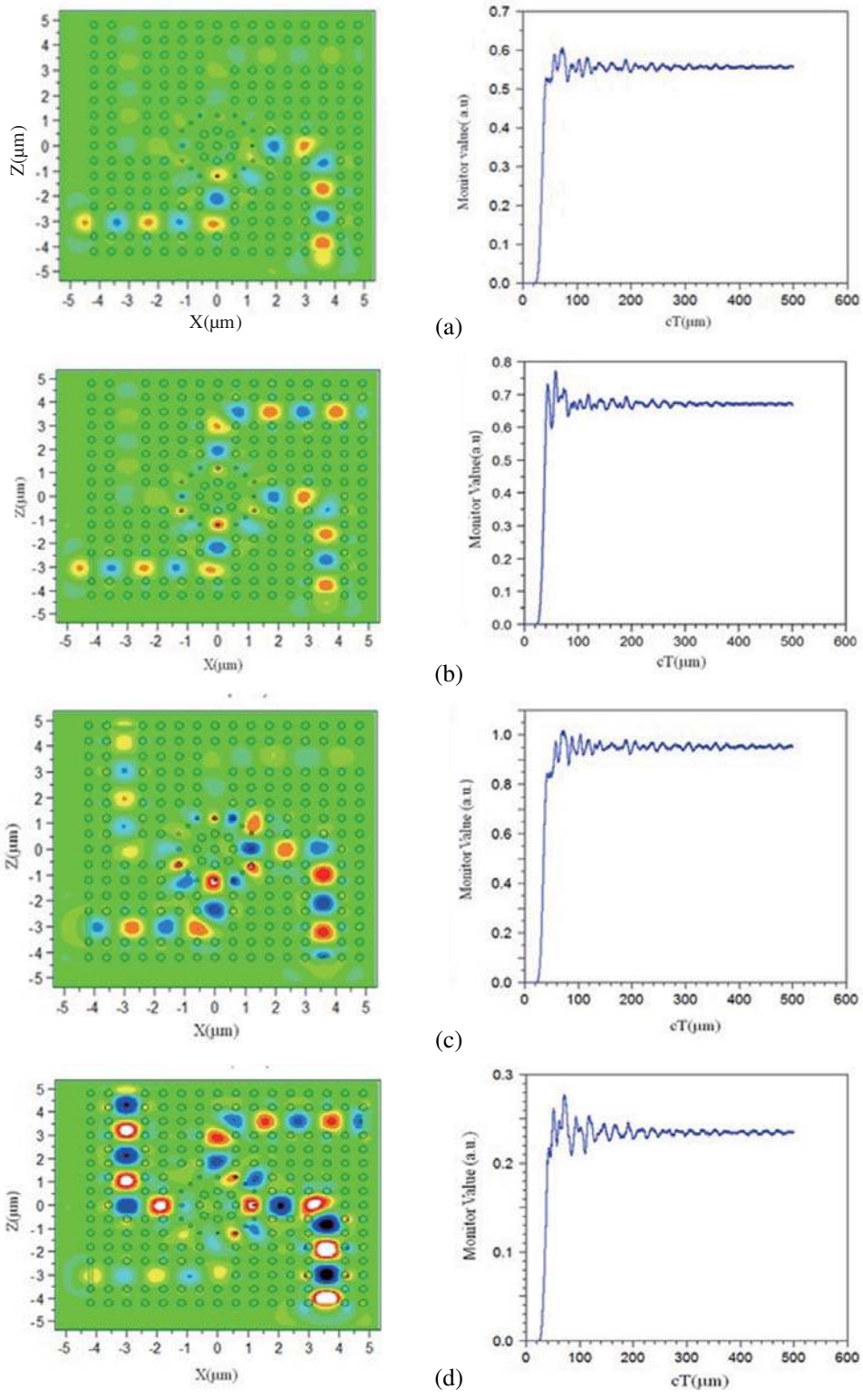

Figure 3. Transmission diagram and output power for the optical NAND gate. (a) $A = 0$, $B = 0$, $CI = 1$, (b) $A = 0$, $B = 1$, $CI = 1$, (c) $A = 1$, $B = 0$, $CI = 1$, (d) $A = 1$, $B = 1$, $CI = 1$.

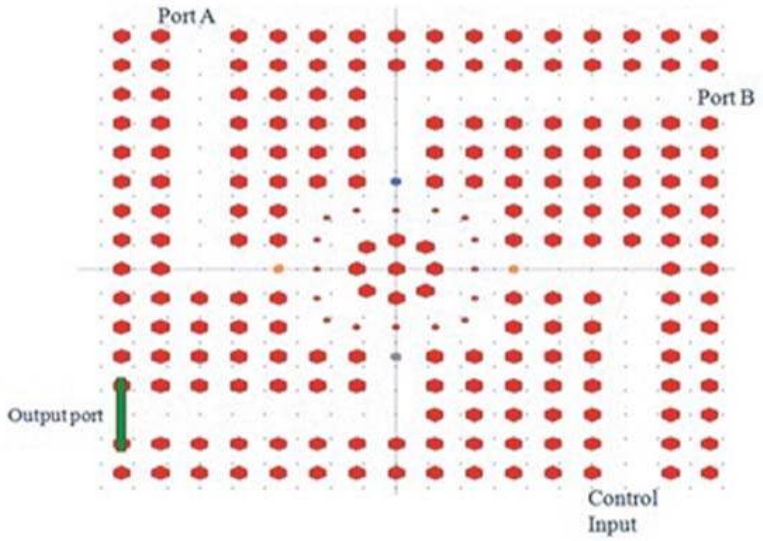

Figure 4. Proposed structure for optical NOR gate.

phase difference of 270 is given to get the desired output. When both the inputs are given, CI is OFF, and the phase for both the inputs is 270. The truth table for optical NOR gate is shown in Table 2.

The transmission diagram and the output powers for the combinations '00', '01' '10', and '11' are shown in Fig. 5. When there is no signal for the combination '00', only the control input is active with the phase difference of 270. Phase difference is applied to get the desired output. The logic output of $0.552P_a$ is obtained and regarded as logic-1. For the combination '01', signal is applied only at port B, and the control input is inactive. The logic output of $0.0105P_a$ is obtained and regarded as logic-0. For the combination '10', the signal is applied at port A, and the control input is inactive. The logic

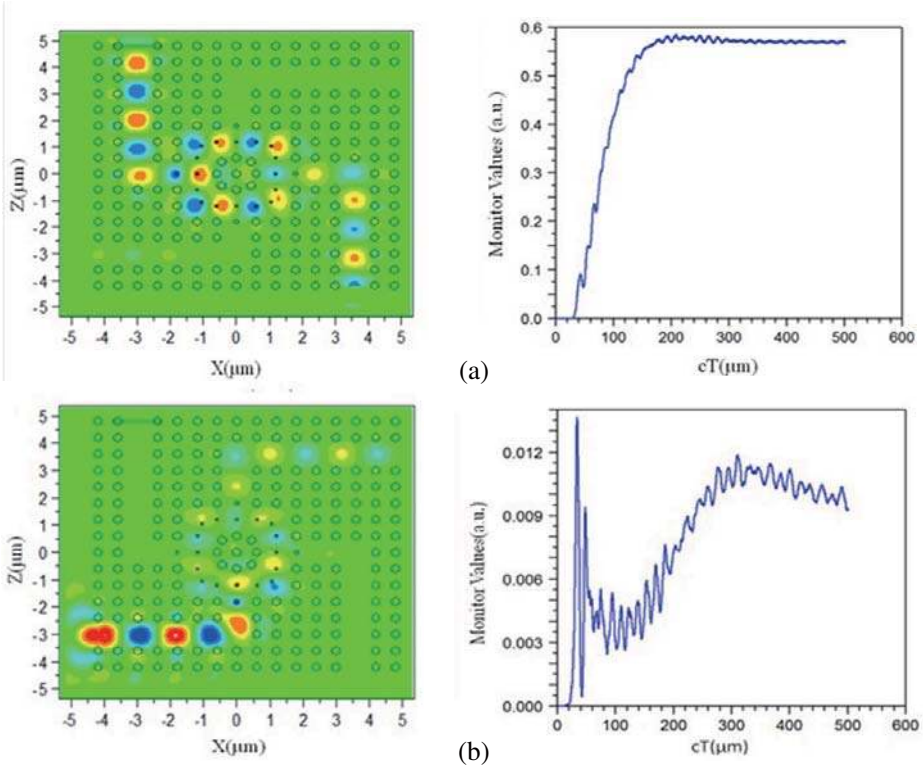

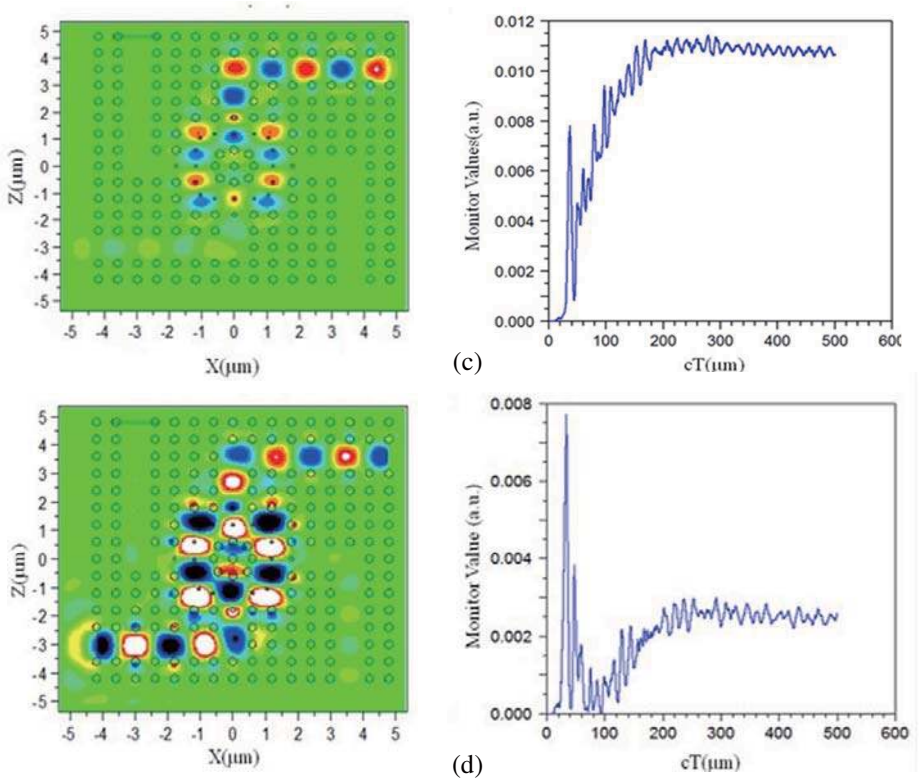

Figure 5. Transmission diagram and the output power for the optical NOR gate. (a) $A = 0$, $B = 0$, $CI = 1$, (b) $A = 0$, $B = 1$, $CI = 0$, (c) $A = 1$, $B = 0$, $CI = 0$, (d) $A = 1$, $B = 1$, $CI = 0$.

output of $0.0107P_a$ is obtained and regarded as logic-0. The signals are given for the combination '11' from both the input ports, and the control input is inactive. The logic output of $0.0130P_a$ is obtained and regarded as logic-0.

In EX-OR gate, the structure has three inputs and one output. The proposed structure is shown in Fig. 6. The resonator part has two rings, outer square shapes ring and inner circular ring. The outer ring which has orange colour rods with the radius of $0.01a$ and the inner ring with the radius of $0.2a$. The blue colour rod in the input port 'B' acts as a scatter rod with the radius of $0.09a$. The square-shaped outer ring rods act as coupling rods to couple the signal in the resonator. The control input is not active for the combination '11'. The applied phase difference for the inputs and CI is given in the table. The phase values are adjusted to get the desired output. The truth table for the EX-OR gate is tabulated in Table 2.

The transmission diagram and the output power for the EX-OR gate are shown in Fig. 7. When the signal is applied to the combination '00', the logic output of $0.351P_a$ is obtained and viewed as

Table 2. Truth table for the proposed universal gates.

Inputs		EX-NOR gate			NAND gate			NOR gate			EX-OR gate		
A	B	CI	Logic O/P	Proposed O/P	CI	Logic O/P	Proposed O/P	CI	Logic O/P	Proposed O/P	CI	Logic O/P	Proposed O/P
0	0	1	1	0.64	1	1	0.558	1	1	0.552	1	0	0.351
0	1	0	0	0.0632	1	1	0.672	0	0	0.0105	1	1	0.575
1	0	0	0	0.12	1	1	0.952	0	0	0.0107	1	1	0.6
1	1	1	1	1.20	1	0	0.234	0	0	0.0130	0	0	0.13

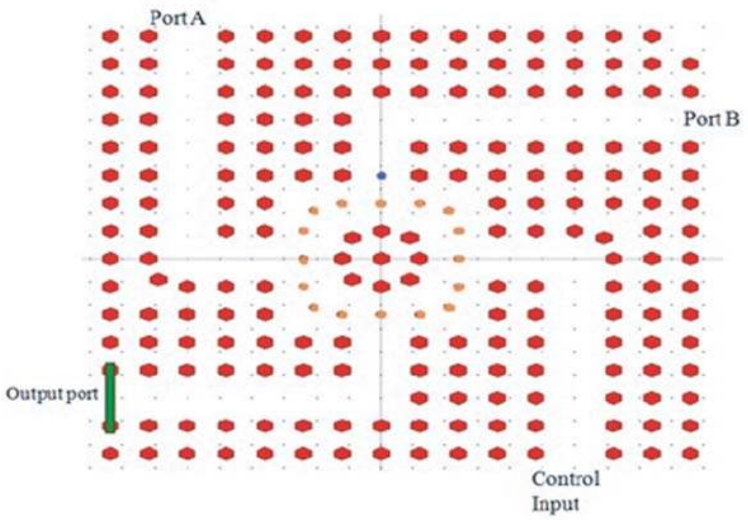

Figure 6. Proposedoptical EX-OR gate structure.

logic-0. For the combination '01', $0.577P_a$ is obtained, and it is viewed as logic-1. The signal for the combination '10' is applied, and the logic output of $0.6P_a$ is obtained and viewed as logic-1. When the signal is applied to the combination '11', the logic output of $0.13P_a$ is obtained and viewed as logic-0. The control input is active for the combinations '00', '01', '10'. The phase difference is applied to the input ports and control inputs to get the desired output. The output power for all the combinations for optical EX-OR is shown in Table 2.

In EX-NOR gate, the proposed structure has three inputs (Port A, Port B and Control input) and

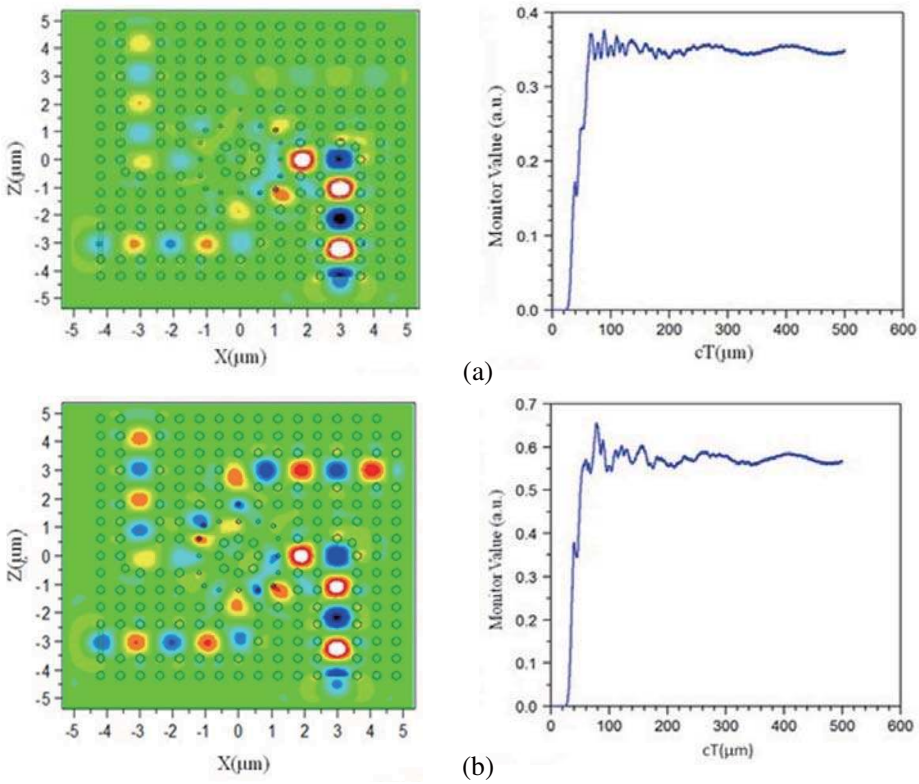

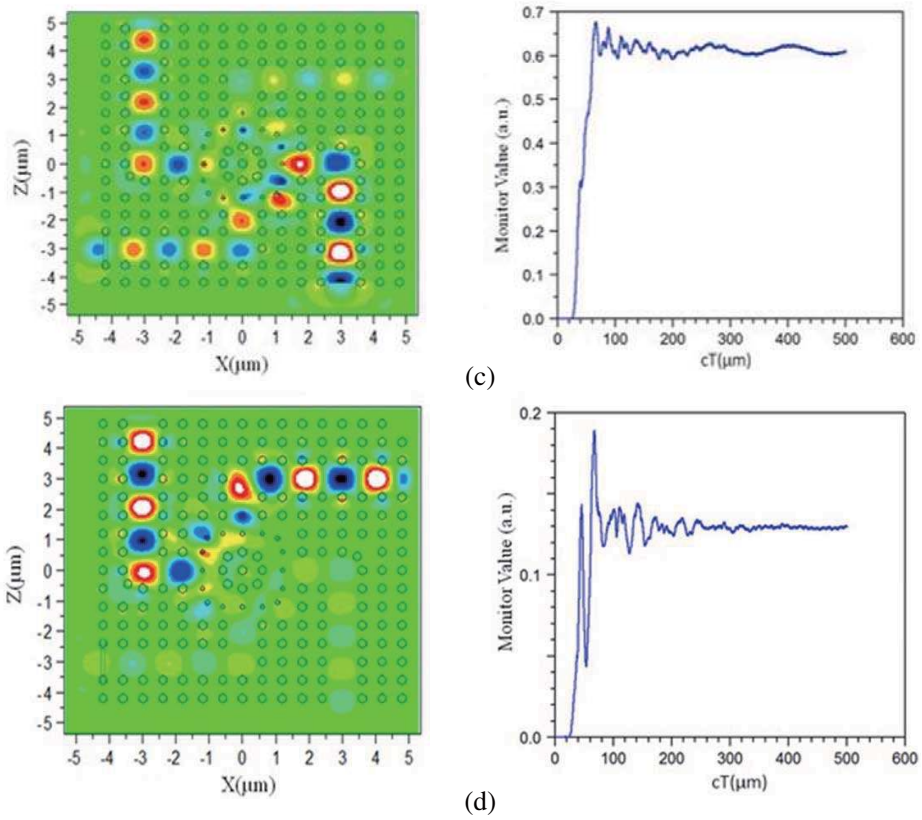

Figure 7. Transmission diagram and the output power for the optical EX-OR gate. (a) $A = 0$, $B = 0$, $CI = 1$, (b) $A = 0$, $B = 1$, $CI = 1$, (c) $A = 1$, $B = 0$, $CI = 1$, (d) $A = 1$, $B = 1$, $CI = 0$.

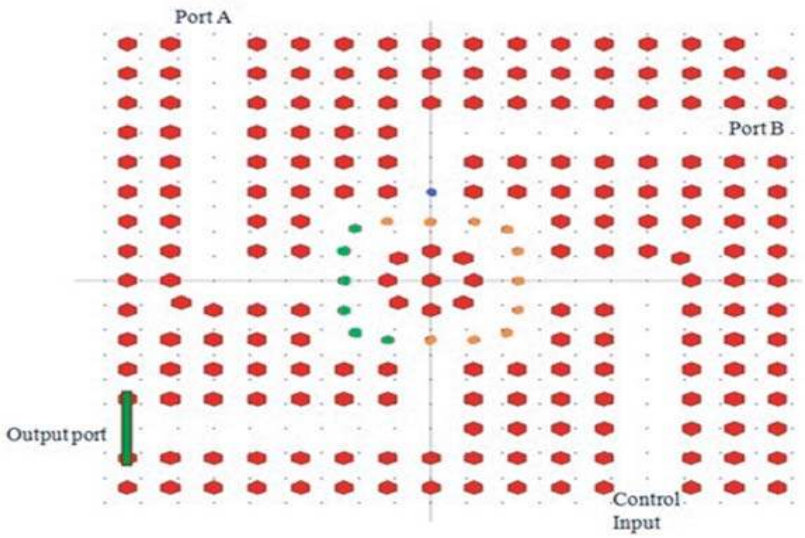

Figure 8. Proposed structure of optical EX-NOR gate.

one output. The structures for the EX-OR and EX-NOR are same. The radius of the resonator alone varies to get the desired output. The CI is not active all the time. CI is active only for certain conditions with some phase shift. The phase shift is applied only to get the desired output. The resonator ring has an outer square-shaped ring and inner circular ring. The outer ring has green colour rods in the

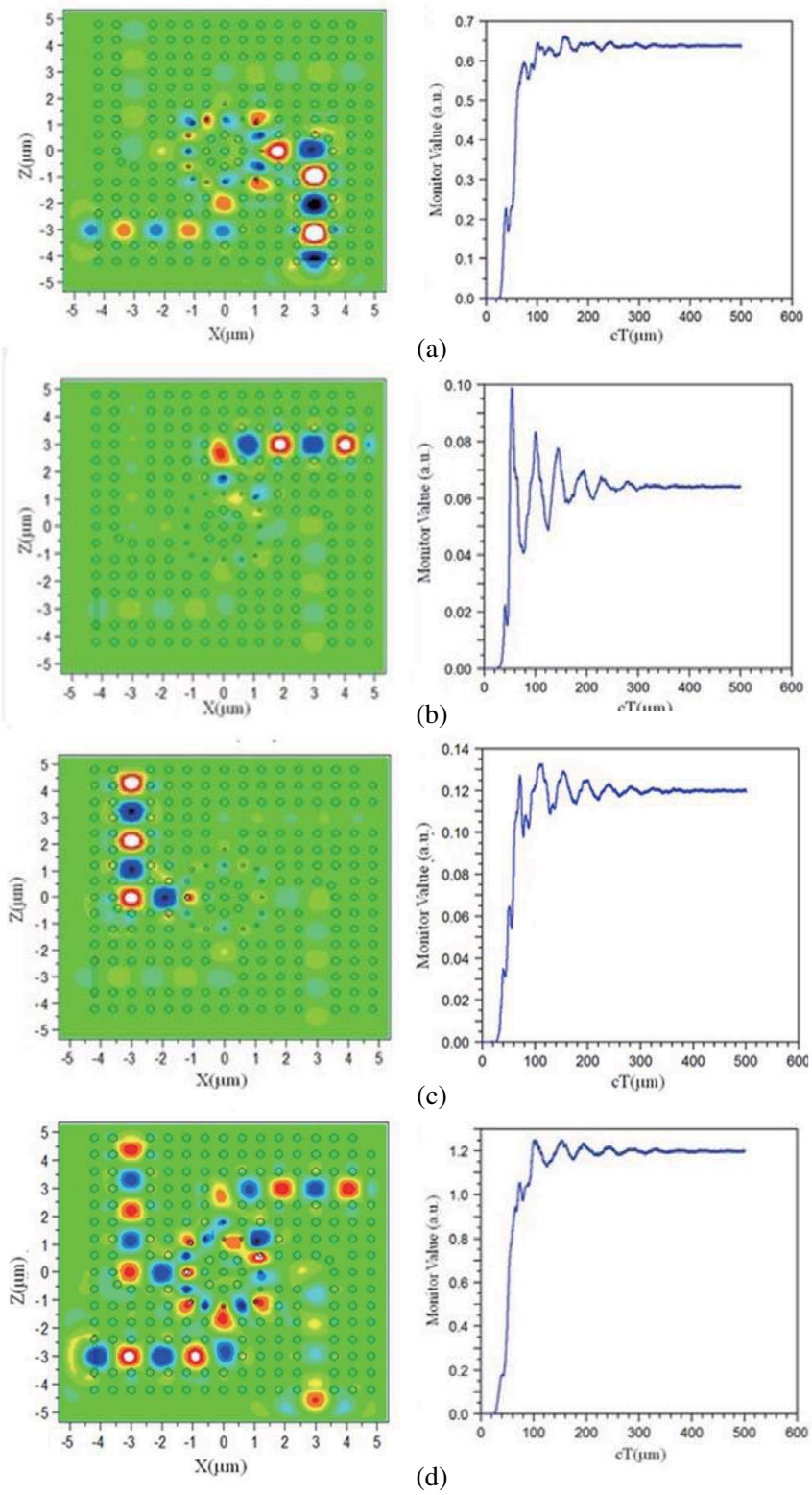

Figure 9. Transmission diagram and the output power for the optical EX-NOR gate. (a) $A = 0$, $B = 0$, $CI = 1$, (b) $A = 0$, $B = 1$, $CI = 0$, (c) $A = 1$, $B = 0$, $CI = 0$, (d) $A = 1$, $B = 1$, $CI = 1$.

resonator with the radius of $0.12a$ and the orange colour rods with the radius of $0.1a$. The single blue rod in the port 'B' has the radius of $0.09a$. The inner circular ring has the radius of $0.2a$. The proposed structure of the gate is shown in Fig. 8.

The transmission diagram and output power for the combinations of the EX-NOR gate are shown in the Fig. 9. The signal is applied to the combination '00', and the logic output of $0.64P_a$ is obtained and viewed as logic-1. For the combination '01', $0.0632P_a$ is obtained and regarded as logic-0. The signal for the combination '10' is applied, and logic output of $0.12P_a$ is obtained and viewed as logic-0. When the signal is applied to the combination '11', the logic output of $1.20P_a$ is obtained and regarded as logic-1. The control input is active for the combinations '00' and '11'. The phase difference is applied to the input ports and control inputs to get the desired output. The output powers for all the combinations are shown in Fig. 9. The truth table for the optical EX-NOR gate is tabulated in Table 2.

4. CONCLUSIONS

This paper discusses the design of a Swastika structured photonic ring crystal with heterogeneous arrangement of two-dimensional photonic crystal for the realization of universal NAND, NOR, EX-OR, and EX-NOR optical gates. The proposed structure finds its application in the design of various modules for telecommunication band as the wavelength of the proposed design is centered at 1550 nm. As the design is compact with good contrast ratio, the proposed design effectively reduces the foot print of optical combinational and sequential circuits.

REFERENCES

1. Yablonovitch, E., "Inhibited spontaneous emission in solid-state physics and electronics," *Phys. Rev. Lett.*, Vol. 58, No. 20, 2059, May 18, 1987.
2. John, S., "Strong localization of photons in certain disordered dielectric superlattices," *Phys. Rev. Lett.*, Vol. 58, No. 23, 2486, Jun. 8, 1987.
3. Goudarzi, K., A. Mir, I. Chaharmahali, and D. Goudarzi, "All-optical XOR and OR logic gates based on line and point defects in 2-D photonic crystal," *Opt & Laser Technol.*, Vol. 1, No. 78, 139-42, Apr. 2016.
4. Fu, Y., X. Hu, and Q. Gong, "Silicon photonic crystal all-optical logic gates," *Phys. Lett. A*, Vol. 377, Nos. 3–4, 329-33, Jan. 3, 2013.
5. D'souza, N. M. and V. Mathew, "Interference based square lattice photonic crystal logic gates working with different wavelengths," *Opt & Laser Technol.*, Vol. 80, 214-9, Jun. 1, 2016.
6. Jiang, Y. C., S. B. Liu, H. F. Zhang, and X. K. Kong, "Reconfigurable design of logic gates based on a two-dimensional photonic crystals waveguide structure," *J. Opt. Commun.*, Vol. 332, 359-65, Dec. 1, 2014.
7. Mohebbi, Z., N. Nozhat, and F. Emami, "High contrast all-optical logic gates based on 2D nonlinear photonic crystal," *J. Opt. Commun.*, Vol. 355, 130-6. Nov. 15, 2015.
8. Fasihi, K., "Design and simulation of linear logic gates in the two-dimensional square-lattice photonic crystals," *Optik*, Vol. 127, No. 11, 4669-74, Jun. 1, 2016.
9. Bchir, R., A. Bardaoui, and H. Ezzaouia, "Design of silicon-based two-dimensional photonic integrated circuits: XOR gate," *IET Optoelectronics*, Vol. 7, No. 1, 25-9, Feb. 1, 2013.
10. Mahmoud, M. Y., G. Bassou, A. Taalbi, and Z. M. Chekroun, "Optical channel drop filters based on photonic crystal ring resonators," *Opt. Commun.*, Vol. 285, No. 3, 368-72, Feb. 1, 2012.
11. Taalbi, A., G. Bassou, and M. Y. Mahmoud, "New design of channel drop filters based on photonic crystal ring resonators," *Opt-Int. J. for Light and Electron Opt.*, Vol. 124, No. 9, 824-7, May 1, 2013.
12. Djavid, M., F. Monifi, A. Ghaffari, and M. S. Abrishanmian, "Hetrostructure wavelength division multiplixers using photonic crystals ring resonators," *Opt. Commun.*, Vol. 28, 4028–4032, 2008.
13. Gupta, M. M. and S. Medhekar, "A versatile optical junction using photonic band-gap guidance and self collimation," *Appl. Phys. Lett.*, Vol. 105, No. 13, 131104, Sep. 29, 2014.

14. Gupta, M. M. and S. Medhekar, "Asymmetric light reflection at the reflecting layer incorporated in a linear, time-independent and non-magnetic two-dimensional photonic crystal," *Eur. Phys. Lett.*, Vol. 114, No. 5, 54002, Jul. 8, 2016.
15. Kannaiyan, V., R. Savarimuthu, and S. K. Dhamodharan, "Performance analysis of an eight channel demultiplexer using a 2D-photonic crystal quasi square ring resonator," *Opto-Electron. Rev.*, Vol. 25, No. 2, 74-9, Jun. 1, 2017.
16. Seifouri, M., S. Olyaee, M. Sardari, and A. Mohebzadeh-Bahabady, "Ultra-fast and compact all-optical half adder using 2D photonic crystals," *Optoelectronics*, Vol. 13, No. 3, 139-43, Jan. 24, 2019.
17. Hassangholizadeh-Kashtiban, M., H. Alipour-Banaei, and M. B. Tavakoli, "Sabbaghi-Nadooshan R. An ultra fast optical reversible gate based on electromagnetic scattering in nonlinear photonic crystal resonant cavities," *J. Opt. Mat.*, Vol. 94, 371-7, Aug. 1, 2019.
18. Khosroabadi, S., A. Shokouhmand, and S. Marjani, "Full optical 2-bit analog to digital convertor based on nonlinear material and ring resonators in photonic crystal structure," *Optik.*, Vol. 200, 163393, Jan. 1, 2020.
19. Zhang, X. R., J. P. Liu, H. Liu, Q. Pan, F. Q. Yang, S. Q. Zhang, Y. M. Guo, X. J. Liu, and X. Y. Wu, "The adjustable band gap structure and transmission characteristics for the two-dimensional function photonic crystal waveguide," *Phys. B: Condensed Matter.*, Vol. 567, 5–10, Aug. 15, 2019.
20. Yee, K., "Numerical solution of initial boundary value problems involving Maxwell's equations in isotropic media," *IEEE Transactions on Antennas and Propagation*, Vol. 14, No. 3, 302–307, 1966.
21. Taflove, A. and M. E. Brodwin, "Numerical solution of steady-state electromagnetic scattering problems using the time-dependent Maxwell's equations," *IEEE Transactions on Microwave Theory and Techniques*, Vol. 23, No. 8, 623–630, 1975.